

Assessment of tumor heterogeneity in treatment-naïve adrenocortical cancer patients using ^{18}F -FDG positron emission tomography

Rudolf A. Werner^{1,2} · Matthias Kroiss^{3,4} · Masatoyo Nakajo^{1,2} · Dirk O. Mügge⁵ · Stefanie Hahner⁴ · Martin Fassnacht^{3,4} · Andreas Schirbel¹ · Christina Bluemel¹ · Takahiro Higuchi^{1,2} · Laszlo Papp⁶ · Norbert Zsótér⁶ · Andreas K. Buck^{1,2} · Ralph A. Bundschuh⁷ · Constantin Lapa¹

Abstract As an orphan malignancy, only limited treatment options are available in adrenocortical carcinoma (ACC). Non-invasive risk assessment has not been described but may be of value to stratify patients for treatment. We aimed to evaluate the potential value of intra-individual tumor heterogeneity as assessed by ^{18}F -fluorodeoxyglucose (^{18}F -FDG) positron emission tomography/computed tomography (PET/CT) for outcome prediction in treatment-naïve ACC patients. Ten patients with primary diagnosis of ACC were included in this study. Prior to any treatment initiation, baseline ^{18}F -FDG PET scans were performed. Tumor staging was performed using the European Network for the Study of Adrenal Tumors (ENS@T). Intratumoral heterogeneity of the primary tumor was assessed by manual segmentation using conventional PET parameters

(standardized uptake values and tumor-to-liver ratios) and textural features. The impact of tumoral heterogeneity based on pre-therapeutic ^{18}F -FDG PET to predict progression-free (PFS) and overall survival (OS) was evaluated by receiver operating characteristic analysis. On average, tumor recurrence or progression was detected after median of 561 days (range 71–1434 days) after the pre-therapeutic baseline PET scan. 50 % of the patients died of ACC within the follow-up period (mean 983 ± 404 days). Pre-therapeutic tumor volume was associated with PFS ($r = -0.67$, $p = 0.05$) and Ki67 index with OS ($r = -0.66$, $p = 0.04$). ENS@T tumor stage was the only parameter to correlate with both PFS and OS ($r = -0.82$, $p = 0.001$, and $r = -0.72$, $p = 0.01$, respectively). In the subgroup of patients without distant metastases (ENS@T stages II and III), age and pre-therapeutic tumor volume correlated significantly with PFS ($r = 0.96$, $p = 0.01$ and $r = -0.93$, $p = 0.02$, respectively) and OS ($r = 0.95$, $p = 0.02$ and $r = -0.90$, $p = 0.04$, respectively). None of the investigated classic or textural PET parameters predicted PFS or OS. In this pilot study in treatment-naïve ACC patients, conventional ^{18}F -FDG PET-derived parameters and textural tumor heterogeneity features were not suitable to identify high-risk patients.

Ralph A. Bundschuh and Constantin Lapa have contributed equally to this work.

✉ Ralph A. Bundschuh
ralph.bundschuh@ukb.uni-bonn.de

- ¹ Department of Nuclear Medicine, University Hospital Würzburg, Würzburg, Germany
- ² Comprehensive Heart Failure Center, University Hospital Würzburg, Würzburg, Germany
- ³ Department of Internal Medicine I, Division of Endocrinology and Diabetes, University Hospital Würzburg, Würzburg, Germany
- ⁴ Comprehensive Cancer Center Mainfranken, University of Würzburg, Würzburg, Germany
- ⁵ University of Applied Science, Hamburg, Germany
- ⁶ Mediso Medical Imaging Systems Ltd., Budapest, Hungary
- ⁷ Department of Nuclear Medicine, University Hospital Bonn, Sigmund-Freud-Strasse 25, 53127 Bonn, Germany

Keywords ACC · Tumor heterogeneity · FDG PET · Textural features

Introduction

Adrenocortical cancer (ACC) is a rare, but highly aggressive tumor entity occurring at any age with a dismal prognosis [1–4]. Open adrenalectomy remains the gold

Table 1 Overview of selected textural parameters

Parameter	Order	Description
Coefficient of variation, COV	1st	A normalized measure of dispersion of a frequency distribution.
Skewness	1st	A measure for the extent to which a frequency distribution “leans” to side of the mean value of the distribution.
Contrast	2nd	Measures the difference of the gray value from voxel to the next voxel. It increases in case of intensity changes between voxels.
Homogeneity	2nd	A measure for continuous areas of same or similar voxel values in an image or voxel of interest.
Entropy	2nd	Measures grade of derangement, e.g., a homogenous matrix demonstrates low entropy.
Short zone emphasis, SZE	3rd	Measures the distribution of short zones. It is highly dependent on occurrence of small zones and is expected to be large for fine textures.
Size zone variability, SZV	3rd	Describes the variation in the size of different substructures in an image (VOI): in case of all subareas of different intensities are 1 voxel size, the size zone variability is low.

standard in local, non-metastatic cases [5]. In those undergoing complete resection, there is a high risk of recurrence up to 80 % [6].

Mitotane (1,1-dichloro-2-(o-chlorophenyl)-2-(p-chlorophenyl)ethane; o,p'-DDD), an adrenolytic compound with specific adrenocortical activity [7], is used as a monotherapy both in an adjuvant setting and in metastatic disease [8, 9]. However, objective tumor response to mitotane alone is observed in only 20 % of patients with advanced disease [10] and hence, more intensive treatment is often required. Cytotoxic chemotherapy of combined etoposide, doxorubicin, cisplatin, and mitotane (EDP-M) has been shown to result in longer progression-free survival (PFS) compared to streptozotocin in a phase III clinical trial [11, 12]. Therefore, EDP-M is now recommended as first-line chemotherapy after mitotane failure [5]. Second-line treatment options have been studied in phase II clinical trials only which include the combination of gemcitabine and capecitabine [13]. Identification of patients with aggressive tumors entailing a high risk of recurrence and rapid tumor progression would be of great value to stratify for more intensive treatment.

¹⁸F-fluorodeoxyglucose (FDG) positron emission/computed tomography (PET/CT) is widely used in the diagnostic work-up of adrenal masses and it has proven its value in ACC staging [14–18]. However, conventional PET parameters like standardized uptake values (SUV) have failed to provide prognostic information [14, 19, 20].

Tumor heterogeneity may be considered to be a relevant predictor of prognosis and treatment response for several reasons. First, heterogeneity may be associated with variable degrees of tumor differentiation and reflect more aggressive biology. Second, glucose uptake in ACC may vary depending on the expression of glucose transporters such as GLUT1/GLUT3 [21].

This suggests a demand for novel strategies to assess outcome prediction beyond simple FDG uptake values. Recently, PET-based assessment of tumor heterogeneity

(so-called textural features) has been demonstrated as a reliable tool for risk stratification in thyroid and rectum cancer [22, 23]. In the present study, we aimed to elucidate the potential of tumor heterogeneity determined by ¹⁸FDG PET/CT of the primary tumor in treatment-naïve ACC patients to predict prognosis.

Materials and methods

Patients

Ten consecutive treatment-naïve patients (2 females, 8 males; mean age 50 ± 14 years, median 51 years, range 17–67 years) with newly diagnosed ACC or adrenal lesions suspicious for ACC were enrolled. ¹⁸F-FDG PET/CT was performed for staging prior to treatment initiation. Only patients with primary diagnosis of ACC prior to initiation of any therapeutic procedure were eligible for this study.

All patients gave written and informed consent to the diagnostic and therapeutic procedures. The European Network for the Study of Adrenal Tumors (ENS@T) staging system was applied [24]. For this observational cohort study, data were retrieved from the German ACC Registry and ENS@T Registry (www.ensat.org/registry) which were approved by the local ethics committee (Approval No. 86/03, 88/11).

Clinical parameters including age at primary diagnosis, pre-therapeutic tumor volume, mean tumor size of resected tumor, hormonal activity of the tumors (plasma and urine metanephrines), and proliferation index (Ki67) were recorded.

All patients were followed up clinically and by imaging (Fig. 1). Progression-free survival (PFS) was defined in accordance to Response Evaluation Criteria in Solid Tumors (RECIST) by serial radiological assessment starting from the time point of baseline imaging [25]. For overall survival (OS), the time interval between baseline PET and the date of death was calculated.

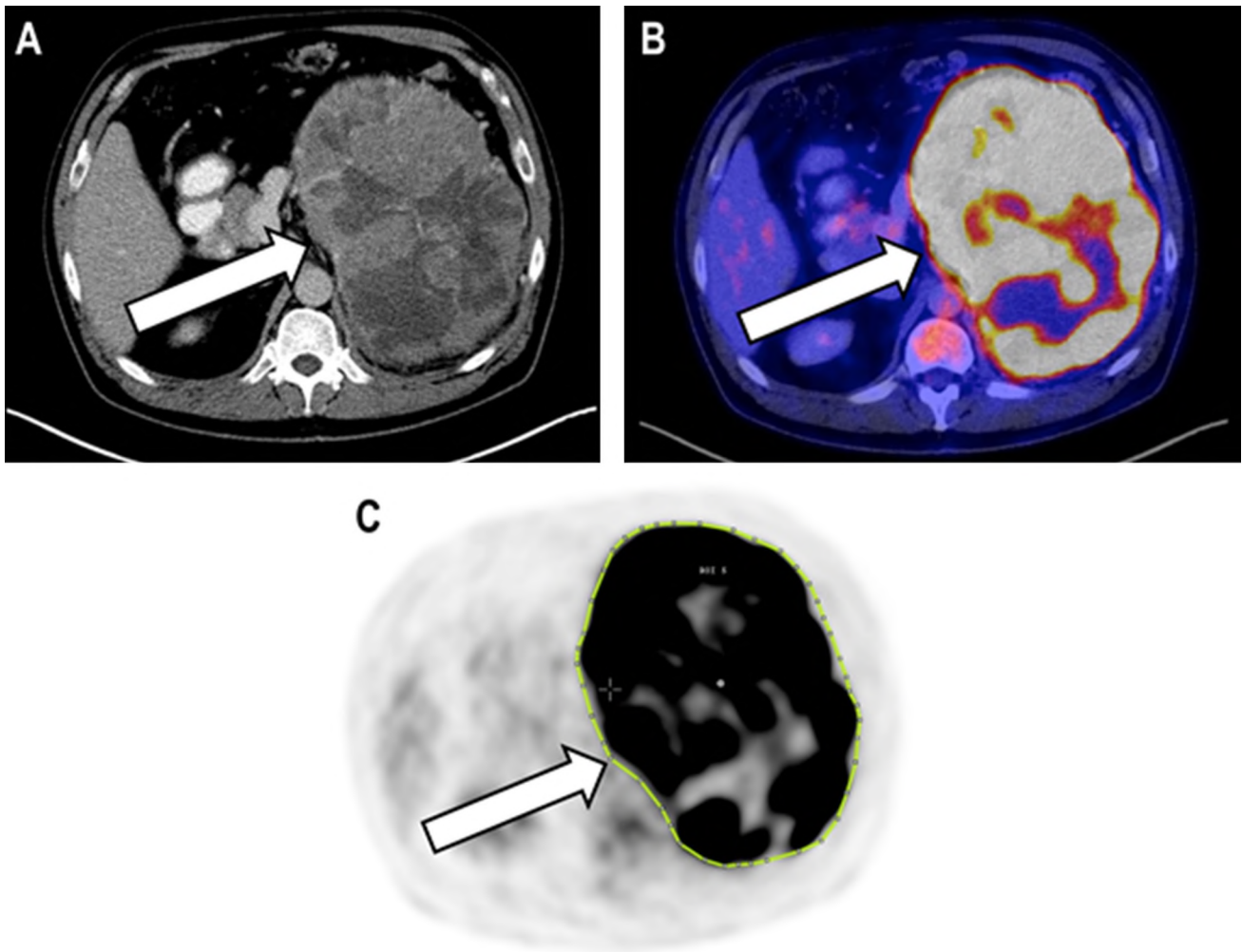


Fig. 1 ^{18}F -fluorodeoxyglucose (^{18}F -FDG) positron emission tomography/computed tomography (PET/CT) of a 52-year-old male patient suffering from ACC (patient #4). The primary tumor can be detected on CT (a) and on ^{18}F -FDG PET/CT (b) indicated by the arrows.

Imaging: ^{18}F -FDG PET/CT

Integrated PET/CT using a Biograph mCT 64 PET/CT scanner (Siemens, Knoxville, USA) consisting of a Lutetium oxyorthosilicate full-ring PET and a 64-slice spiral CT was performed in all patients. ^{18}F -FDG (339 ± 33 MBq) was injected intravenously at a glucose level of 80 ± 10 mg/dl. After a waiting time of 63 ± 4 min, transmission data using spiral CT with (80 mAs, 120 kV, a 512×512 matrix, 5-mm slice thickness, $n = 7$) or without (40 mAs, 120 kV, a 512×512 matrix, 5 mm slice thickness) contrast enhancement ($n = 3$, due to renal impairment) including the base of the skull to the proximal thighs were conducted. Consecutively, PET emission data were acquired in three-dimensional mode with a 200×200 matrix. After decay and scatter correction, PET data were reconstructed iteratively

with attenuation correction, using the algorithm implemented by the manufacturer. Manual stepwise segmentation of the primary (arrow) by a region of interest on the PET-only images was performed (c). An overview of investigated heterogeneity parameters can be found in [26], Tables 1 and 3

with attenuation correction, using the algorithm implemented by the manufacturer.

Image and data analysis

Imaging data were analyzed using an Interview Fusion Workstation (Mediso Medical Imaging Systems Ltd., Budapest, Hungary). The primary tumor was manually segmented using combined PET/CT data side-by-side (Fig. 1). Apart from conventional PET parameters, several different textural parameters were evaluated for assessment of textural heterogeneity which were classified as *first-order parameters* [e.g., coefficient of variation (COV) and skewness], *second-order parameters* (entropy, homogeneity, correlation, and contrast) and *higher order parameters* (e.g., size zone variability, intensity variability, short zone emphasis, long zone emphasis, and low gray-level zone

emphasis). A detailed description of selected textural parameters can be found in [26] and Table 1. Conventional diagnostic parameters were also evaluated, such as maximum standardized uptake values (SUV_{max}), peak SUV (SUV_{peak}), and mean liver uptake ($LIVER_{mean}$). Semi-quantitative analysis for derivation of those PET parameters was performed by selecting the axial PET image slice displaying the maximum primary tumor uptake by drawing a 3D volume of interest (VOI) around the whole tumor area. Tumor regions of interest (ROIs) were defined in two ways. First, a standardized 15-mm circular region was placed over the area with the peak activity. This first ROI was used to derive maximum (SUV_{max}) and mean standardized uptake values (SUV_{peak}). A reference region was defined by drawing a ROI (diameter of 50 mm) involving normal liver parenchyma ($LIVER_{mean}$) to derive tumor-to-liver ratios. Tumor-to-liver ratios for SUV_{max} and SUV_{peak} were calculated. The radiotracer concentration in the ROIs was normalized to the injected dose per kilogram of patient's body weight to derive the SUVs.

Statistical analysis

Statistical analysis was performed using SPSS Statistics 22 as previously described [22]. Clinical and imaging parameters were correlated with OS and PFS using Pearson correlation analysis. A two-sided t test was used to test whether the correlation was statistically significant within a 95 % confidence level. The cutoff values of each parameter for the prediction of PFS and OS were determined by means of receiver operating characteristic (ROC) analysis. Therefore, the Youden index was used to maximize the sum of sensitivity and specificity [27]. For AUCs, exact binominal confidence intervals were calculated (95 % confidence level), indicating the statistical significance of predictive capability if the critical value of 0.5 is not included. Kaplan–Meier analysis was performed using thresholds established before by ROC analysis. Non-parametric log-rank tests were used to assess the differences in the Kaplan–Meier curves and differences with a *p* value < 0.05 were considered significant.

Analysis was primarily performed for the whole group. In a second step, patients were divided into two subgroups comprising patients (a) without (ENS@T stages II and III; group 1) and (b) with distant metastases (ENS@T stage IV; group 2).

Results

Patients

ACC was histologically confirmed in all patients by tumor biopsy or surgery. Two patients were classified as ENS@T

stage II, three as ENS@T stage III, and five as ENS@T stage IV. Sites of metastases included bone and liver in three patients each, lung in two, and distant abdominal lymph nodes in one patient.

7/10 (70 %) patients presented with hormonally active disease. Six patients underwent surgery with a complete resection in five patients. Resected tumors had a mean size of 16.2 ± 7.2 cm (median 14.5 cm, range 5.5–25 cm). Proliferation index Ki67 ranged from 2 to 50 % (median 20 %).

6/10 (60 %) patients underwent tumor surgery which constituted the only therapy in patient #5. For systemic treatment, 2/10 (20 %) subjects received mitotane alone which was followed by radiation therapy. 5/10 (50 %) patients were treated with EDP-M. The remaining two patients received chemotherapy with vincristine/doxorubicin and carboplatin/etoposide followed by mitotane consolidation. 5/10 (50 %) were treated in a palliative setting.

Within follow-up (2834 days), 7/10 (70 %) suffered from progressive disease with a PFS of 736 ± 551 days (range 71–1434 days, median 561 days). The remaining 3/10 (30 %) patients (patients #3, #5, #7) could be classified as stable disease. 5/10 (50 %) patients (patients #1, #4, #6, #8, #10) died from their cancer (983 ± 404 days, range 378–1434 days, median 1080 days) with 4/5 initially suffering from ENS@T stage IV disease.

Patients' characteristics can be found in Table 2.

PET imaging

^{18}F -FDG PET scans were positive in all subjects. The SUV_{max} of the primary tumor was 20.8 ± 13.8 (median 15.7, range 10.8–46.6); the SUV_{peak} was 13.6 ± 7.6 (median 10.5, range 7.5–28.0) with a $LIVER_{mean}$ of 2.1 ± 0.3 (median 2.2, range 1.53–2.41). Tumor-to-liver ratios were 10.3 ± 7.4 (median 7.6, range 4.9–26.8, for SUV_{max}) and 6.7 ± 4.1 (median 5.3, range 3.8–16.1, for SUV_{peak}), respectively.

Correlation of clinical, textural, and PET parameters with PFS (whole cohort)

Pre-therapeutic primary tumor volume and ENS@T stage correlated with disease-free survival (tumor volume, $r = -0.67$, $p = 0.05$; ENS@T, $r = -0.82$, $p = 0.001$). None of the other investigated clinical, textural, or PET parameters revealed potential to predict PFS.

Correlation of clinical, textural, and PET parameters with OS (whole cohort)

ENS@T stage and Ki67 were the only parameters to significantly correlate with OS ($r = -0.72$, $p = 0.01$ and

Table 2 Patients' characteristics

Case	Sex	Age	Resection margin	Size of primary (cm)	Ki67 %	ENS@T classification	Hormonal activity	Sites of metastases	Initial treatment	Subsequent/second-line treatment	Progression-free survival (days)	Overall survival (days)
#1	f	64	n/a	12	n/a	4	Yes	Lung, bone	Mitotane, RTx	None	71	416
#2	m	50	R1	5.5	2	2	No	None	Surgery	Mitotane, RTx	1261	1302 ^b
#3	m	46	R0	12	20	3	Yes	None	EDP-M	Surgery	1263 ^a	1263 ^b
#4	m	52	n/a	25	10	4	Yes	Bone	EDP-M	None	294	779
#5	m	60	R0	12.5	12	2	Yes	None	Surgery	None	1413 ^a	1413 ^b
#6	m	17	R0	30	n/a	3	Yes	None	Surgery	Mitotane, vincristine/doxorubicin/ ifosfamide	285	900
#7	f	48	R0	15	20	3	No	None	Surgery	Carboplatin/etoposide, mitotane	1434 ^a	1434 ^b
#8	m	43	R0	21	20	4	Yes	Liver	Surgery	EDP-M	386	683
#9	m	57	n/a	15	n/a	4	No	Bone, liver	EDP-M	None	736	1259 ^b
#10	m	67	n/a	14	50	4	Yes	Lymph nodes, liver, lung	EDP-M	None	215	378

f female, m male, ENS@T European Network for the Study of Adrenal Tumors, EDP-M combination regimen of etoposide, doxorubicin, cisplatin and mitotane, RTx radiation therapy

^a No disease progression/recurrence at date of data censoring

^b Alive at date of data censoring

Table 3 Overview of selected investigated parameters and corresponding *r* and *p* values for the whole cohort and ENS@T group I (stages II, III)

Parameter	Progression-free survival		Overall survival	
	<i>r</i> value	<i>p</i> value	<i>r</i> value	<i>p</i> value
<i>Clinical parameters, conventional PET parameters, and PET-derived textural features were correlated with PFS and OS for the whole cohort</i>				
Clinical parameters				
Age	0.02	0.9	−0.2	0.6
Ki67 (%)	−0.49	0.2	−0.66	0.04*
Hormonal activity	0.02	0.95	−0.18	0.6
Conventional parameters				
SUV _{max}	−0.41	0.3	−0.46	0.2
SUV _{peak}	−0.48	0.2	−0.51	0.1
<i>T</i> _{max} to liver	−0.46	0.2	−0.47	0.2
<i>T</i> _{peak} to liver	−0.53	0.1	−0.51	0.1
Pre-therapeutic tumor volume	−0.67	0.05*	−0.43	0.2
Textural features				
ENS@T	−0.82	0.001*	−0.72	0.01*
COV	−0.29	0.4	−0.2	0.5
Skewness	0.02	0.9	−0.01	0.9
Contrast	−0.44	0.2	−0.44	0.2
Homogeneity	0.05	0.9	0.19	0.6
Entropy	−0.58	0.9	−0.43	0.2
SZE	0.03	0.9	−0.16	0.7
SZV	0.33	0.4	0.34	0.3
<i>Clinical parameters, conventional PET parameters, and PET-derived textural features were correlated with PFS and OS for ENS@T group I (stages II, III)</i>				
Clinical parameters				
Age	0.96	0.01*	0.95	0.02*
Ki67 (%)	0.38	0.5	0.2	0.7
Hormonal activity	−0.41	0.5	−0.45	0.4
Conventional parameters				
SUV _{max}	0.56	0.3	0.56	0.3
SUV _{peak}	0.26	0.7	0.16	0.8
<i>T</i> _{max} to liver	−0.11	0.9	−0.04	0.9
<i>T</i> _{peak} to liver	−0.65	0.2	−0.67	0.2
Pre-therapeutic tumor volume	−0.93	0.02*	−0.90	0.04*
Textural features				
COV	0.13	0.8	−0.0025	0.9
Skewness	0.18	0.8	0.01	0.9
Contrast	−0.04	0.9	−0.14	0.8
Homogeneity	−0.36	0.5	−0.48	0.4
Entropy	−0.5	0.4	−0.45	0.4
SZE	0.56	0.3	0.67	0.2
SZV	−0.8	0.8	−0.14	0.8

Correlation of clinical parameters (age, Ki67, hormonal activity, ENS@T), conventional positron emission tomography (PET) parameters (SUV_{max}, SUV_{peak}, *T*_{max} to liver, *T*_{peak} to liver) and PET-based heterogeneity parameters [COV, skewness, contrast, homogeneity, entropy, short zone emphasis (SZE), size zone variability (SZV)] with progression-free and overall survival (for whole cohort and ENS@T group I)

PFS progression-free survival, *OS* overall survival, *ENS@T* European Network for the Study of Adrenal Tumors, *SUV* standardized uptake value, *T*_{max} to liver tumor-to-liver ratios for SUV_{max}, *T*_{peak} to liver tumor-to-liver ratios for SUV_{peak}, *COV* coefficient of Variation, *SZE* short zone emphasis, *SZV* size zone variability

* Reached statistical significance

$r = -0.66$, $p = 0.04$, respectively). All other clinical or imaging-derived features failed to reach statistical significance.

Correlation of clinical, textural, and PET parameters with PFS/OS according to ENS@T stage

According to ENS@T stage, patients were sub-divided in two groups: Group I comprised ENS@T II and III patients (5/10 (50 %)), whereas group II consisted of subjects with distant metastases (ENS@T IV, 5/10 (50 %)).

For group I, age and pre-therapeutic tumor volume correlated significantly with PFS ($r = 0.96$, $p = 0.01$ and $r = -0.93$, $p = 0.02$, respectively) and OS ($r = 0.95$, $p = 0.02$ and $r = -0.90$, $p = 0.04$, respectively).

For group II, no significant correlation could be demonstrated.

An overview of selected investigated parameters and corresponding r and p values for the whole cohort and for ENS@T group I is given in Table 3.

Discussion

In this pilot study comprising 10 patients with newly diagnosed, treatment-naïve ACC, the potential of ^{18}F -FDG PET/CT at diagnosis prior to any treatment was evaluated. In addition to conventional PET parameters and clinical features, textural parameters were analyzed by PET-based assessment of primary tumor heterogeneity.

Due to its ability to visualize whole-body metabolism, PET is a powerful tool in the diagnostic work-up of adrenal masses [14, 18]. The prognostic capability of PET-based tumor heterogeneity has been demonstrated in several tumor entities, such as thyroid cancer, rectal cancer, non-small cell lung cancer, or high-grade gliomas [22, 23, 28, 29]. Additionally, ACC itself often presents as a heterogeneous tumor including necrotic areas and varying tomographic densities. Therefore, we hypothesized that assessment of intratumoral heterogeneity might provide additional information for risk stratification in ACC patients at initial staging.

However, none of the investigated PET-derived standard parameters like SUV or tumor-to-liver ratios or textural parameters was significantly associated with disease-free or overall survival. ^{18}F -FDG PET is known as a useful tool for staging and restaging purposes in the work-up of ACC patients [15–17] and has been shown to detect metastatic sites which were missed by other imaging modalities [30]. In line with a previous study by Tessonnier et al. [14], ^{18}F -FDG uptake (SUV_{max}) was not correlated with outcome in our patient population. In contrast, Leboulloux et al. [18]

reported that the intensity of ^{18}F -FDG uptake is related to survival in ACC patients. However, its usefulness as an independent prognostic factor or for therapeutic management was not analyzed.

In our cohort, pre-therapeutic primary tumor volume was correlated with disease-free survival and Ki67 proliferation index with overall survival, which is in line with previous findings by Libé et al. [31]. ENS@T stage was the only parameter to significantly correlate with both PFS and OS. In the subgroup of patients without distant metastases, age and tumor volume could be demonstrated to be correlated with PFS and OS. Beyond tumor stage, none of the parameters examined was correlated with prognosis in ENS@T stage IV patients. Given the intrinsic heterogeneity of ACC itself as expressed by inhomogeneous presentation in morphologic and functional imaging due to the initial presence of necrosis, inter-individual differences in primary tumor ^{18}F -FDG uptake may be only minor. Other targets to identify high-risk patients are to be further investigated. For example, ^{68}Ga -Pentixafor, a radiolabeled cyclic pentapeptide with high affinity to chemokine receptor CXCR4, has recently been developed [32–34]. Proof-of-concept for visualization of CXCR4-expression has been demonstrated in patients with hematologic malignancies [35, 36], glioblastoma [37], and after myocardial infarction [38, 39]. Since CXCR4 has been reported to be overexpressed in ACC [40], evaluation of tumoral receptor expression on the tumor cell surface might be a new target worth further assessment.

This study has some limitations. First, reproducibility of PET/CT parameters assumed to reflect tumor heterogeneity has not finally been demonstrated. However, Tixier et al. [41] were able to demonstrate reproducibility of textural features comparable to classic PET parameters in a recent study. Since all ACC in our cohort were relatively large tumors (Fig. 1), we assume that partial volume effects can be neglected. Manual tumor segmentation as performed in our study might be more reliable in accurate assessment of tumor borders in PET images than semi-automatic methods which might fail depending on the tumor localization [42, 43].

Second, statistical power is limited due to the small sample size. However, ACC is a rare disease with an annual incidence of less than 2 new cases per million [44, 45] and we were able to enroll a homogeneous cohort of patients with treatment-naïve, newly diagnosed disease. Additionally, this is an observational analysis in only one center and hence selection bias cannot be excluded. Collaborative efforts within academic networks such as ENS@T may permit acquisition of larger numbers of cases to clarify a potential value of PET/CT-based assessment of tumor heterogeneity.

Conclusion

In this pilot study in treatment-naïve ACC patients, conventional ¹⁸F-FDG PET-derived parameters and textural tumor heterogeneity features were not suitable to identify high-risk patients.

Authors' contributions RAW, CL, MK, and RAB contributed to conception and design. CL, RAW, DOM, MK, AS, MN, and CB acquired, analyzed, and interpreted the data. CL, RAW, RAB, and DOM drafted the manuscript. MF, SH, TH, and AKB revised it critically. NZ and LP implemented the heterogeneity parameter in the beta version of the software. All authors read and approved the final manuscript.

Compliance with ethical standards

Conflict of interest All authors had full control of the data and information submitted for publication. RB has a non-commercial research contract with Mediso Medical Imaging Systems, RB is on the speaker's bureau for Mediso Medical Imaging Systems, and LP and NZ are employed by Mediso Medical Imaging Systems. No potential conflicts of interest were disclosed by the other authors.

References

1. K.Y. Bilimoria, W.T. Shen, D. Elaraj, D.J. Bentrem, D.J. Winchester, E. Kebebew, C. Sturgeon, Adrenocortical carcinoma in the United States: treatment utilization and prognostic factors. *Cancer* **113**(11), 3130–3136 (2008). doi:10.1002/ncr.23886
2. A. Berruti, E. Baudin, H. Gelderblom, H.R. Haak, F. Porpiglia, M. Fassnacht, G. Pentheroudakis, ESMO Guidelines Working Group, Adrenal cancer: ESMO Clinical Practice Guidelines for diagnosis, treatment and follow-up. *Ann. Oncol.* **23**(Suppl 7), vii131–138 (2012). doi:10.1093/annonc/mds231
3. T. Else, A.C. Kim, A. Sabolch, V.M. Raymond, A. Kandathil, E.M. Caoili, S. Jolly, B.S. Miller, T.J. Giordano, G.D. Hammer, Adrenocortical carcinoma. *Endocr. Rev.* **35**(2), 282–326 (2014). doi:10.1210/er.2013-1029
4. M. Fassnacht, R. Libe, M. Kroiss, B. Allolio, Adrenocortical carcinoma: a clinician's update. *Nat. Rev. Endocrinol.* **7**(6), 323–335 (2011). doi:10.1038/nrendo.2010.235
5. M. Fassnacht, M. Kroiss, B. Allolio, Update in adrenocortical carcinoma. *J. Clin. Endocrinol. Metab.* **98**(12), 4551–4564 (2013). doi:10.1210/jc.2013-3020
6. R.F. Pommier, M.F. Brennan, An eleven-year experience with adrenocortical carcinoma. *Surgery* **112**(6), 963–970 (1992)
7. S. Sbiera, E. Leich, G. Liebisch, I. Sbiera, A. Schirbel, L. Wiemer, S. Matysik, C. Eckhardt, F. Gardill, A. Gehl, S. Kendl, I. Weigand, M. Bala, C.L. Ronchi, T. Deutschbein, G. Schmitz, A. Rosenwald, B. Allolio, M. Fassnacht, M. Kroiss, Mitotane Inhibits Sterol-O-Acyl transferase 1 triggering lipid-mediated endoplasmic reticulum stress and apoptosis in adrenocortical carcinoma cells. *Endocrinology* **156**(11), 3895–3908 (2015). doi:10.1210/en.2015-1367
8. M. Fassnacht, B. Allolio, Clinical management of adrenocortical carcinoma. *Best Pract. Res. Clin. Endocrinol. Metab.* **23**(2), 273–289 (2009). doi:10.1016/j.beem.2008.10.008
9. D. Bergenstal, M. Lipsett, R. Moy, R. Hertz, Regression of adrenal cancer and suppression of adrenal function in men by O, p'DDD. *Trans. Am. Phys.* **72**, 341 (1959)
10. S. De Francia, A. Ardito, F. Daffara, B. Zaggia, A. Germano, A. Berruti, F. Di Carlo, Mitotane treatment for adrenocortical carcinoma: an overview. *Minerva Endocrinol.* **37**(1), 9–23 (2012)
11. A. Berruti, E. Baudin, H. Gelderblom, H.R. Haak, F. Porpiglia, M. Fassnacht, G. Pentheroudakis, E.G.W. Grp, Adrenal cancer: ESMO Clinical Practice Guidelines for diagnosis, treatment and follow-up. *Ann. Oncol.* **23**, 131–138 (2012). doi:10.1093/annonc/mds231
12. M. Fassnacht, M. Terzolo, B. Allolio, E. Baudin, H. Haak, A. Berruti, S. Welin, C. Schade-Brittinger, A. Lacroix, B. Jarzab, H. Sorbye, D.J. Torpy, V. Stepan, D.E. Scheingart, W. Arlt, M. Kroiss, S. Leboulleux, P. Sperone, A. Sundin, I. Hermsen, S. Hahner, H.S. Willenberg, A. Tabarin, M. Quinkler, C. de la Fouchardiere, M. Schlumberger, F. Mantero, D. Weismann, F. Beuschlein, H. Gelderblom, H. Wilmink, M. Sender, M. Edgerly, W. Kenn, T. Fojo, H.H. Muller, B. Skogseid, FIRM-ACT Study Group, Combination chemotherapy in advanced adrenocortical carcinoma. *N. Engl. J. Med.* **366**(23), 2189–2197 (2012). doi:10.1056/NEJMoa1200966
13. P. Sperone, A. Ferrero, F. Daffara, A. Priola, B. Zaggia, M. Volante, D. Santini, B. Vincenzi, G. Badalamenti, C. Intrivici, S. Del Buono, S. De Francia, E. Kalomirakis, R. Ratti, A. Angeli, L. Dogliotti, M. Papotti, M. Terzolo, A. Berruti, Gemcitabine plus metronomic 5-fluorouracil or capecitabine as a second-/third-line chemotherapy in advanced adrenocortical carcinoma: a multi-center phase II study. *Endocr. Relat. Cancer* **17**(2), 445–453 (2010). doi:10.1677/ERC-09-0281
14. L. Tessonnier, C. Ansquer, C. Bournaud, F. Sebag, E. Mirallie, J.C. Lifante, F.F. Palazzo, I. Morange, D. Drui, C. de la Fouchardere, J. Mancini, D. Taieb, F-18-FDG uptake at initial staging of the adrenocortical cancers: a diagnostic tool but not of prognostic value. *World J. Surg.* **37**(1), 107–112 (2013). doi:10.1007/s00268-012-1802-y
15. S. Takeuchi, A. Balachandran, M.A. Habra, A.T. Phan, R.L. Bassett Jr, H.A. Macapinlac, H.H. Chuang, Impact of (1)(8)F-FDG PET/CT on the management of adrenocortical carcinoma: analysis of 106 patients. *Eur. J. Nucl. Med. Mol. Imaging* **41**(11), 2066–2073 (2014). doi:10.1007/s00259-014-2834-3
16. D. Deandreis, S. Leboulleux, C. Caramella, M. Schlumberger, E. Baudin, FDG PET in the management of patients with adrenal masses and adrenocortical carcinoma. *Horm. Cancer* **2**(6), 354–362 (2011). doi:10.1007/s12672-011-0091-5
17. G.C. Mackie, B.L. Shulkin, R.C. Ribeiro, F.P. Worden, P.G. Gauger, R.J. Mody, L.P. Connolly, G. Kunter, C. Rodriguez-Galindo, J.W. Wallis, C.A. Hurwitz, D.E. Scheingart, Use of [18F]fluorodeoxyglucose positron emission tomography in evaluating locally recurrent and metastatic adrenocortical carcinoma. *J. Clin. Endocrinol. Metab.* **91**(7), 2665–2671 (2006). doi:10.1210/jc.2005-2612
18. S. Leboulleux, C. Dromain, G. Bonniaud, A. Auperin, B. Caillou, J. Lumbroso, R. Sigal, E. Baudin, M. Schlumberger, Diagnostic and prognostic value of 18-fluorodeoxyglucose positron emission tomography in adrenocortical carcinoma: a prospective comparison with computed tomography. *J. Clin. Endocrinol. Metab.* **91**(3), 920–925 (2006). doi:10.1210/jc.2005-1540
19. K. Satoh, D. Patel, W. Dieckmann, N. Nilubol, E. Kebebew, Whole body metabolic tumor volume and total lesion glycolysis predict survival in patients with adrenocortical carcinoma. *Ann. Surg. Oncol.* **22**(Suppl 3), 714–720 (2015). doi:10.1245/s10434-015-4813-8
20. A. Cistaro, A. NiccoliAsabella, P. Coppolino, N. Quartuccio, C. Altini, M. Cucinotta, P. Alongi, M. Balma, S. Sanfilippo, A. Buschiazzo, A. Piccardo, M. Fanelli, G. Sambuceti, J. Bomanji, S. Baldari, G. Bisi, S. Fanti, G. Rubini, Diagnostic and prognostic value of 18F-FDG PET/CT in comparison with morphological

- imaging in primary adrenal gland malignancies—a multicenter experience. *Hell. J. Nucl. Med.* **18**(2), 97–102 (2015). doi:[10.1967/s002449910202](https://doi.org/10.1967/s002449910202)
21. W. Fenske, H.U. Volker, P. Adam, S. Hahner, S. Johanssen, S. Wortmann, M. Schmidt, M. Morcos, H.K. Muller-Hermelink, B. Allolio, M. Fassnacht, Glucose transporter GLUT1 expression is an stage-independent predictor of clinical outcome in adrenocortical carcinoma. *Endocr. Relat. Cancer* **16**(3), 919–928 (2009). doi:[10.1677/ERC-08-0211](https://doi.org/10.1677/ERC-08-0211)
 22. C. Lapa, R.A. Werner, J.S. Schmid, L. Papp, N. Zsoter, J. Biko, C. Reiners, K. Herrmann, A.K. Buck, R.A. Bundschuh, Prognostic value of positron emission tomography-assessed tumor heterogeneity in patients with thyroid cancer undergoing treatment with radiopeptide therapy. *Nucl. Med. Biol.* **42**(4), 349–354 (2015). doi:[10.1016/j.nucmedbio.2014.12.006](https://doi.org/10.1016/j.nucmedbio.2014.12.006)
 23. R.A. Bundschuh, J. Dinges, L. Neumann, M. Seyfried, N. Zsoter, L. Papp, R. Rosenberg, K. Becker, S.T. Astner, M. Henninger, K. Herrmann, S.I. Ziegler, M. Schwaiger, M. Essler, Textural parameters of tumor heterogeneity in (1)(8)F-FDG PET/CT for therapy response assessment and prognosis in patients with locally advanced rectal cancer. *J. Nucl. Med.* **55**(6), 891–897 (2014). doi:[10.2967/jnumed.113.127340](https://doi.org/10.2967/jnumed.113.127340)
 24. M. Fassnacht, S. Johanssen, M. Quinkler, P. Bucszy, H.S. Willenberg, F. Beuschlein, M. Terzolo, H.H. Mueller, S. Hahner, B. Allolio, German Adrenocortical Carcinoma Registry Group, European Network for the Study of Adrenal Tumors, Limited prognostic value of the 2004 International Union Against Cancer staging classification for adrenocortical carcinoma: proposal for a Revised TNM Classification. *Cancer* **115**(2), 243–250 (2009). doi:[10.1002/cncr.24030](https://doi.org/10.1002/cncr.24030)
 25. E.A. Eisenhauer, P. Therasse, J. Bogaerts, L.H. Schwartz, D. Sargent, R. Ford, J. Dancey, S. Arbuck, S. Gwyther, M. Mooney, L. Rubinstein, L. Shankar, L. Dodd, R. Kaplan, D. Lacombe, J. Verweij, New response evaluation criteria in solid tumours: revised RECIST guideline (version 1.1). *Eur. J. Cancer* **45**(2), 228–247 (2009). doi:[10.1016/j.ejca.2008.10.026](https://doi.org/10.1016/j.ejca.2008.10.026)
 26. S. Chicklore, V. Goh, M. Siddique, A. Roy, P.K. Marsden, G.J. Cook, Quantifying tumour heterogeneity in 18F-FDG PET/CT imaging by texture analysis. *Eur. J. Nucl. Med. Mol. Imaging* **40**(1), 133–140 (2013). doi:[10.1007/s00259-012-2247-0](https://doi.org/10.1007/s00259-012-2247-0)
 27. W.J. Youden, Index for rating diagnostic tests. *Cancer* **3**(1), 32–35 (1950)
 28. T. Pyka, R.A. Bundschuh, N. Andratschke, B. Mayer, H.M. Specht, L. Papp, N. Zsoter, M. Essler, Textural features in pre-treatment [F18]-FDG-PET/CT are correlated with risk of local recurrence and disease-specific survival in early stage NSCLC patients receiving primary stereotactic radiation therapy. *Radiat. Oncol.* **10**, 100 (2015). doi:[10.1186/s13014-015-0407-7](https://doi.org/10.1186/s13014-015-0407-7)
 29. T. Pyka, J. Gempt, D. Hiob, F. Ringel, J. Schlegel, S. Bette, H.J. Wester, B. Meyer, S. Forster, Textural analysis of pre-therapeutic [18F]-FET-PET and its correlation with tumor grade and patient survival in high-grade gliomas. *Eur. J. Nucl. Med. Mol. Imaging* **43**(1), 133–141 (2016). doi:[10.1007/s00259-015-3140-4](https://doi.org/10.1007/s00259-015-3140-4)
 30. A. Becherer, H. Vierhapper, C. Potzi, G. Karanikas, A. Kurtaran, J. Schmaljohann, A. Staudenherz, R. Dudczak, K. Kletter, FDG-PET in adrenocortical carcinoma. *Cancer Biother. Radiopharm.* **16**(4), 289–295 (2001). doi:[10.1089/108497801753131363](https://doi.org/10.1089/108497801753131363)
 31. R. Libe, I. Borget, C.L. Ronchi, B. Zaggia, M. Kroiss, T. Kerkhofs, J. Bertherat, M. Volante, M. Quinkler, O. Chabre, M. Bala, A. Tabarin, F. Beuschlein, D. Vezzosi, T. Deutschbein, F. Borsion-Chazot, I. Hermsen, A. Stell, C. Fottner, S. Lebouilleux, S. Hahner, M. Mannelli, A. Berruti, H. Haak, M. Terzolo, M. Fassnacht, E. Baudin, ENSAT network, Prognostic factors in stage III-IV adrenocortical carcinomas (ACC): an European Network for the Study of Adrenal Tumor (ENSAT) study. *Ann. Oncol.* **26**(10), 2119–2125 (2015). doi:[10.1093/annonc/mdv329](https://doi.org/10.1093/annonc/mdv329)
 32. O. Demmer, E. Gourni, U. Schumacher, H. Kessler, H.J. Wester, PET imaging of CXCR4 receptors in cancer by a new optimized ligand. *ChemMedChem* **6**(10), 1789–1791 (2011). doi:[10.1002/cmdc.201100320](https://doi.org/10.1002/cmdc.201100320)
 33. K. Herrmann, C. Lapa, H.J. Wester, M. Schottelius, C. Schiepers, U. Eberlein, C. Bluemel, U. Keller, S. Knop, S. Kropf, A. Schirbel, A.K. Buck, M. Lassmann, Biodistribution and radiation dosimetry for the chemokine receptor CXCR4-targeting probe 68Ga-pentixafor. *J. Nucl. Med.* **56**(3), 410–416 (2015). doi:[10.2967/jnumed.114.151647](https://doi.org/10.2967/jnumed.114.151647)
 34. E. Gourni, O. Demmer, M. Schottelius, C. D’Alessandria, S. Schulz, I. Dijkgraaf, U. Schumacher, M. Schwaiger, H. Kessler, H.J. Wester, PET of CXCR4 expression by a (68)Ga-labeled highly specific targeted contrast agent. *J. Nucl. Med.* **52**(11), 1803–1810 (2011). doi:[10.2967/jnumed.111.098798](https://doi.org/10.2967/jnumed.111.098798)
 35. K. Philipp-Abbrederis, K. Herrmann, S. Knop, M. Schottelius, M. Eiber, K. Luckerath, E. Pietschmann, S. Habringer, C. Gerngross, K. Franke, M. Rudelius, A. Schirbel, C. Lapa, K. Schwamborn, S. Steidle, E. Hartmann, A. Rosenwald, S. Kropf, A.J. Beer, C. Peschel, H. Einsele, A.K. Buck, M. Schwaiger, K. Gotze, H.J. Wester, U. Keller, In vivo molecular imaging of chemokine receptor CXCR4 expression in patients with advanced multiple myeloma. *EMBO Mol. Med.* **7**(4), 477–487 (2015). doi:[10.15252/emmm.201404698](https://doi.org/10.15252/emmm.201404698)
 36. H.J. Wester, U. Keller, M. Schottelius, A. Beer, K. Philipp-Abbrederis, F. Hoffmann, J. Simecek, C. Gerngross, M. Lassmann, K. Herrmann, N. Pellegata, M. Rudelius, H. Kessler, M. Schwaiger, Disclosing the CXCR4 expression in lymphoproliferative diseases by targeted molecular imaging. *Theranostics* **5**(6), 618–630 (2015). doi:[10.7150/thno.11251](https://doi.org/10.7150/thno.11251)
 37. C. Lapa, K. Lueckerath, I. Kleinlein, C.M. Monoranu, T. Linsenmann, A.F. Kessler, M. Rudelius, S. Kropf, A.K. Buck, R.I. Ernestus, H.J. Wester, M. Löh, K. Herrmann, 68Ga-Pentixafor-PET/CT for imaging of chemokine receptor 4 expression in glioblastoma. *Theranostics* **6**(3), 428–434 (2016). doi:[10.7150/thno.13986](https://doi.org/10.7150/thno.13986)
 38. J.T. Thackeray, T. Derlin, A. Haghikia, L.C. Napp, Y. Wang, T.L. Ross, A. Schafer, J. Tillmanns, H.J. Wester, K.C. Wollert, J. Bauersachs, F.M. Bengel, Molecular imaging of the chemokine receptor CXCR4 after acute myocardial infarction. *JACC Cardiovasc. Imaging* **8**(12), 1417–1426 (2015). doi:[10.1016/j.jcmg.2015.09.008](https://doi.org/10.1016/j.jcmg.2015.09.008)
 39. C. Lapa, T. Reiter, R.A. Werner, G. Ertl, H.J. Wester, A.K. Buck, W.R. Bauer, K. Herrmann, [68Ga]Pentixafor-PET/CT for imaging of chemokine receptor 4 expression after myocardial infarction—proof-of-concept. *JACC Cardiovasc. Imaging* **8**(12), 1466–1468 (2016). doi:[10.1016/j.jcmg.2015.09.007](https://doi.org/10.1016/j.jcmg.2015.09.007)
 40. K. Lang, A. Stürmer, P. Adam, M. Fassnacht, M. Quinkler, M. Morcos, B. Allolio, S. Hahner, Chemokine receptor expression in the adrenal cortex and in adrenocortical tumours. *Endocrine Abstracts*, 11th European Congress of Endocrinology, vol. 20 (2009), p. P20
 41. F. Tixier, C.C. Le Rest, M. Hatt, N. Albarghach, O. Pradier, J.P. Metges, L. Corcos, D. Visvikis, Intratumor heterogeneity characterized by textural features on baseline 18F-FDG PET images predicts response to concomitant radiochemotherapy in esophageal cancer. *J. Nucl. Med.* **52**(3), 369–378 (2011). doi:[10.2967/jnumed.110.082404](https://doi.org/10.2967/jnumed.110.082404)
 42. H. Zaidi, M. Abdoli, C.L. Fuentes, I.M. El Naqa, Comparative methods for PET image segmentation in pharyngolaryngeal squamous cell carcinoma. *Eur. J. Nucl. Med. Mol. Imaging* **39**(5), 881–891 (2012). doi:[10.1007/s00259-011-2053-0](https://doi.org/10.1007/s00259-011-2053-0)
 43. R.A. Bundschuh, N. Andratschke, J. Dinges, M.N. Duma, S.T. Astner, M. Brugel, S.I. Ziegler, M. Molls, M. Schwaiger, M. Essler, Respiratory gated [18F]FDG PET/CT for target volume delineation in stereotactic radiation treatment of liver metastases.

- Strahlenther. Onkol. **188**(7), 592–598 (2012). doi:[10.1007/s00066-012-0094-3](https://doi.org/10.1007/s00066-012-0094-3)
44. S.H. Golden, K.A. Robinson, I. Saldanha, B. Anton, P.W. Ladenson, Clinical review: prevalence and incidence of endocrine and metabolic disorders in the United States: a comprehensive review. *J. Clin. Endocrinol. Metab.* **94**(6), 1853–1878 (2009). doi:[10.1210/jc.2008-2291](https://doi.org/10.1210/jc.2008-2291)
45. T.M.A. Kerkhofs, R.H.A. Verhoeven, J.M. Van der Zwan, J. Dieleman, M.N. Kerstens, T.P. Links, L.V. Van de Poll-Franse, H.R. Haak, Adrenocortical carcinoma: a population-based study on incidence and survival in the Netherlands since 1993. *Eur. J. Cancer* **49**(11), 2579–2586 (2013). doi:[10.1016/j.ejca.2013.02.034](https://doi.org/10.1016/j.ejca.2013.02.034)